CERAMICI PE BAZĂ DE SnO₂ PENTRU SENZORI DE GAZ
SnO₂ BASED CERAMICS FOR GAS SENSORS

ANDREI-DAN BUSUIOC, RAMONA ENUŢĂ, ŞTEFANIA STOLERIU ∗, TEODOR VIŞAN
University POLITEHNICA of Bucharest, RO-011061, Bucharest, Romania

Pure and La^{3+} or V^{5+} doped SnO_2 based ceramics were obtained by shaping and sintering of nanosized powders, previously synthesized by the precipitation method. The thermal treatment temperature was in the 1300 - 1500°C range. The resulted ceramic bodies were characterized through X-ray diffraction and scanning electron microscopy coupled with energy-dispersive X-ray spectroscopy. The ceramic properties and sensitivity towards methane and isopropyl alcohol vapours were also determined. It was demonstrated that dopants use has a beneficial effect on the gas detection capability, especially at low concentrations.

Ceramicile pe bază de SnO_2 pur şi dopat cu La^{3+} sau V^{5+} au fost obţinute prin fasonarea şi sinterizarea unor pulberi nanometrice, sintetizate anterior prin metoda precipitării. Temperatura de tratament termic a fost cuprinsă în intervalul 1300 - 1500°C. Corpurile ceramice rezultate au fost caracterizate prin intermediul difracţiei de raze X şi a microscopiei electronice cu baleiaj cuplate cu spectroscopie de raze X cu dispersie după energie. De asemenea, au fost determinate proprietăţile ceramice şi sensibilitatea faţă de metan şi vapori de alcool izopropilic. S-a demonstrat că utilizarea dopanţilor are un efect favorabil asupra capacităţii de detecţie a gazelor, mai ales la concentraţii mici.

Keywords: Tin Oxide; Semiconductor; Ceramics; Dopants; Gas Sensitivity.

1. Introduction

The sudden and massive losses of hazardous gases endanger the lives of employees in industrial plants, but also that of residents in their own homes [1]; on a larger scale, the uncontrolled leaks of toxic gases can affect the environment [2], with repercussions on the entire ecosystem. These are the reasons why the fabrication and commercialisation, but also performance improvement of gas sensors represents a major concern of the present [3, 4]. The researchers focused on the development of extremely sensitive and selective devices [5, 6], with an indisputable accent on the domain of semiconductors, such as: SnO_2 [7, 8], ZnO [9], TiO_2 [10], In_2O_3 [11] etc. There are three key factors that should be considered when designing a gas sensor: the receptor function, played by the surface of each oxide grain, the transducer function, played by each grain boundary, and the utility factor, governed by the microstructural aspects (high porosity and small dimensions) [12].

Tin dioxide (SnO_2) is a *n* type semiconductor, with a broad direct bandgap of about 3.6 eV [13], and one of the most used due to its chemical stability and mechanical properties [14, 15]. SnO_2 conductivity mainly originates from the oxygen vacancies, defects that lead to non-stoechiometric materials, but also play an important role in the gas sensing mechanism [16]. The unique physical and chemical properties of SnO_2 recommend it for the fabrication of a wide range of devices, with applications in the following fields: sensors [7, 8], solar cells [17], batteries [18], transistors [19], photocatalysts [20], membranes [21] etc.

The properties of SnO_2 based gas sensors can be improved either by increasing the material specific surface for a better gas - surface interaction [22] or by introducing doping elements to modify the material conductivity [23]. Thus, it has been reported that the gas detection capability of the corresponding ceramics is strongly dependent on their morphology [24] and considerable efforts have been made to synthesize various nanostructures [25, 26]. Moreover, the introduction of additional energy levels at the lower edge of the conduction band reduces the energy required for the chemisorption of gas molecules on the semiconductor surface [23, 27].

Many manufacturing methods have been used for the production of gas sensors based on semiconductor metal oxide, but the conventional approaches remain the most embraced at industrial level, even though they suppose high processing temperatures [28]. Nevertheless, the hybrid or non-conventional techniques gained ground lately, showing their huge potential in the optimization of material properties [25, 26, 29].

As mentioned, SnO_2 is mostly employed as doped material [30], the preferred cations being those of the noble metals due to their catalytic

---

character [5]. There are also dopants that inhibit the grain growth, with beneficial effect on the functional characteristics [31, 32]. La^{3+} is a good choice as dopant for SnO_2 since it is a low negativity cation, fact that enhances the sensitivity towards the volatile organic compounds [33]. Moreover, it has already been reported that the use of V^{5+} as dopant, for other type of ceramics, namely $Ba(Mg_{1/3}Ta_{2/3})O_3$ [34, 35]; leads to significant microstructural modifications; in this particular case, it improves SnO_2 sensors performance for low levels of doping [36], due to the existence of vanadium cations with lower valence [37].

In this work, we report on the synthesis and characterization of La^{3+} or V^{5+} doped SnO_2 ceramics. The precursor powders containing 0.5, 1.0 or 2.0 wt.% dopant oxide have been synthesized by the precipitation method, which yields pure, homogenous and nanosized powders. The compositional, structural and morphological modifications generated by the sintering process were investigated, as well as the influence of dopants and thermal history on the gas detection efficiency.

2.Experimental

Pure and doped SnO_2 ceramics were obtained from the powders prepared by the precipitation method, as described in a previous paper [38]. La^{3+} and V^{5+} have been employed as dopants, the selected proportions of the corresponding oxide being 0.5, 1.0 or 2.0 wt.%. The dried precipitates have been calcined at 400°C for 2 h, leading to crystalline SnO_2 phase with tetragonal symmetry. It has been highlighted that the presence of dopants influences both the average crystallite size and bandgap width, the effects being more pronounced for the case of vanadium.

The calcined powders were uniaxially pressed at 150 MPa into disks of 13 mm diameter and about 2 mm height and subsequently sintered at 1300, 1400 or 1500°C for 4 h, in air, with a heating rate of 10°C/min.

The sintered pellets were characterized in terms of apparent density (ρ_a) by employing Arthur method, in xylene. Moreover, X-ray diffraction (XRD), scanning electron microscopy (SEM) coupled with energy-dispersive X-ray spectroscopy (EDX) and electrical measurements were performed on the samples. A Shimadzu XRD 6000 diffractometer with Ni filtered Cu Kα radiation (λ = 0.154 nm) was used to identify the crystalline phases and their structure, 2θ ranging between 20 and 80°, while a Quanta Inspect F scanning electron microscope was employed to visualize the ceramics morphology. Silver contacts were placed on both parallel sides of the disks in order to make possible the measurement of material electrical

resistance both in fresh and contaminated air; the response in the presence of methane or isopropyl alcohol vapours was tested with a Hewlett Packard 4263B LCR Meter station.

3.Results and discussion

The pressed samples were subjected to a sintering process at 1300, 1400 or 1500°C, after which they were characterized in terms of ceramic properties. However, since the most representative parameter is the relative density, Fig. 1 displays its variation as a function of sintering temperature, as well as dopant type and concentration for all prepared pellets. It can be easily noticed that the presence of La^{3+} in any proportion provokes an accentuated decrease of the relative density (Fig. 1a); this may be related to the phenomenon of lanthanum rich compound segregation as a secondary phase, especially at higher dopant concentrations, as it will be shown later (Figs. 2 and 3). In the case of V^{5+} (Fig. 1b), the trend changes, namely the relative density decrease, generated by a small amount of dopant (0.5 wt.%), is followed by a pronounced increase for larger quantities of foreign cations (1.0 and 2.0 wt.%). For both dopants, a minimum of property is recorded for the concentration of 0.5 wt.%, probably due to crystalline network disordering and distortion. As it was expected, the increase of the sintering temperature leads to a better densification of SnO_2 based ceramics.

In order to investigate the evolution of the phase composition, the X-ray diffraction patterns were collected for the thermally treated pellets. Some of these are presented in Fig. 2 and 3, the first one showing the influence of the sintering temperature, while the second focuses on the compositional implications of dopant concentration. Thus, the specimens consist of SnO_2 with tetragonal structure (JCPDS 01-080-6727), as indicated by the intense and narrow diffraction peaks, for which the values of Miller indices were provided. In addition, for the higher sintering temperature and mainly for the higher La^{3+} content, the emergence of a secondary phase can be observed, as it was also evidenced by Mrabet *et al.* [39]; this was identified as $La_2Sn_2O_7$ (JCPDS 00-073-1686). In these conditions, the behaviour of La^{3+} containing ceramics will be affected by the dopant segregation as distinct mineralogical phase distributed in SnO_2 matrix.

Comparing the current results with those reported for the doped SnO_2 powders [38], it can be stated that the thermal treatment promoted the total incorporation of V^{5+} content in the crystalline network, while the effect was completely opposite in the case of La^{3+}, generating a separated lanthanum rich phase. The explanation is based on the ionic radius differences, as follows: 0.690 Å for Sn^{4+}, 1.032 Å for La^{3+} and 0.540 Å for V^{5+}, all
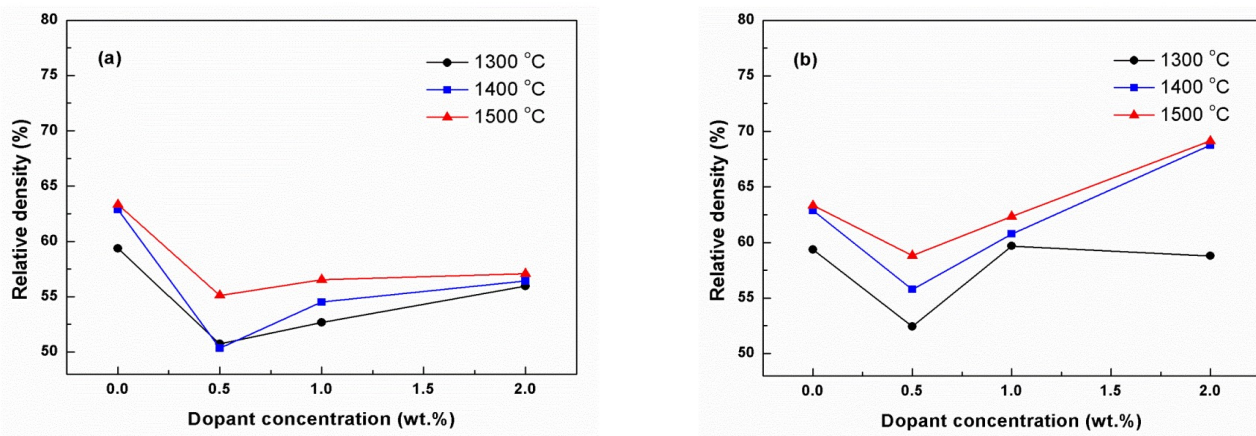
Fig. 1 - Variation of relative density of SnO₂ based ceramics as a function of sintering temperature and dopant quantity for La³⁺ (a) and V⁵⁺ (b) / *Variaţia densităţii relative a ceramicilor pe bază de SnO₂ în funcţie de temperatura de sinterizare şi cantitatea de dopant pentru La³⁺ (a) şi V⁵⁺ (b).*
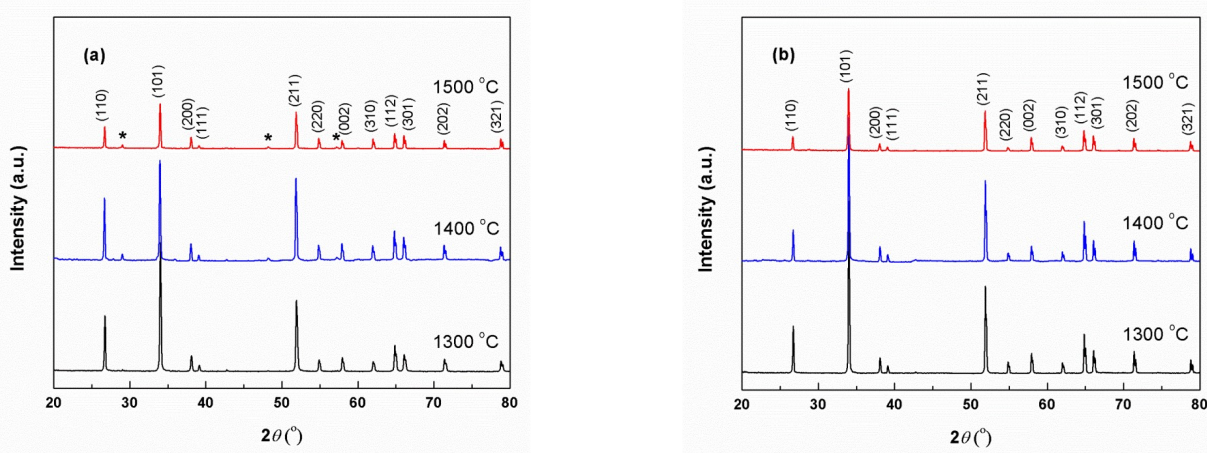

Fig. 2 - XRD patterns for SnO₂ based sintered ceramics and doped with 0.5 wt.% La³⁺ (a) and V⁵⁺ (b). * indicates the secondary phase / *Analizele de difracţie a razelor X pentru ceramicile pe bază de SnO₂ sinterizate şi dopate cu 0,5 % grav. La³⁺ (a) şi V⁵⁺ (b). * indică faza secundară.*
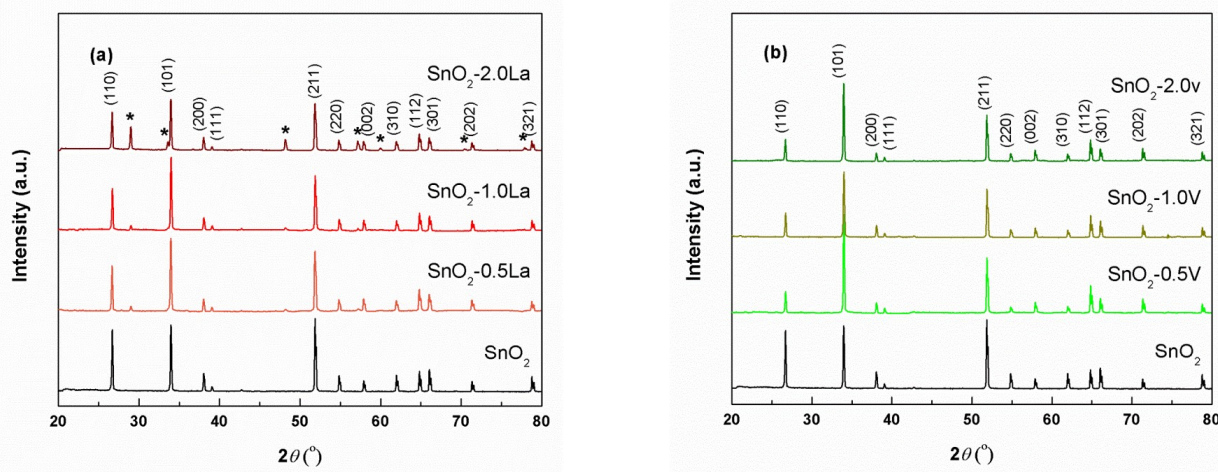

Fig. 3 - XRD patterns for SnO₂ based ceramics sintered at 1400°C and doped with La³⁺ (a) and V⁵⁺ (b). * indicates the secondary phase/ *Analizele de difracţie a razelor X pentru ceramicile pe bază de SnO₂ sinterizate la 1400°C şi dopate cu La³⁺ (a) şi V⁵⁺ (b). * indică faza secundară.*

cations being considered in coordination VI. Thereby, it will be much easier for V⁵⁺ to penetrate the ordered structure of SnO₂ since its ionic radius is closer to that of Sn⁴⁺.

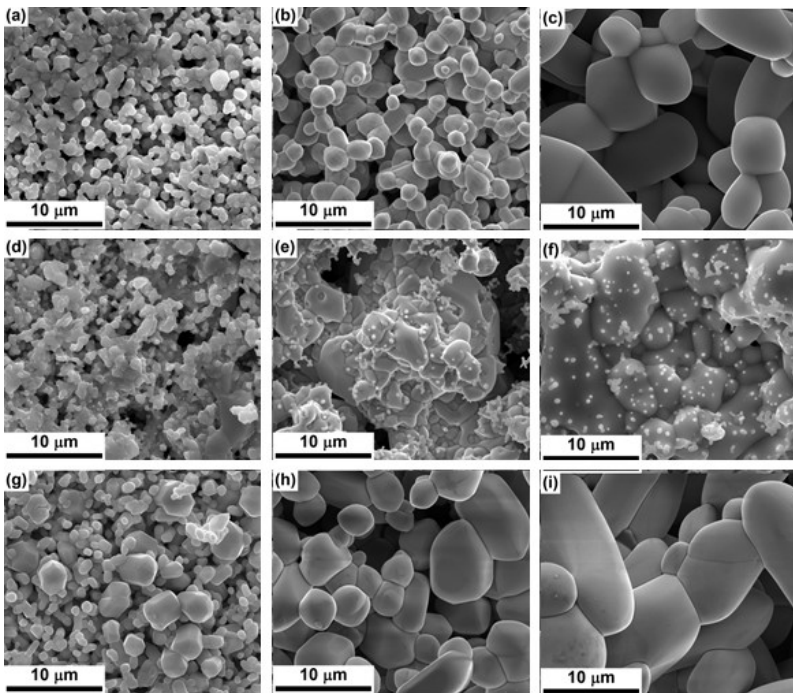Fig. 4 - SEM images of SnO₂ based ceramics sintered at 1300°C (a), 1400°C (b) and 1500°C (c), of SnO₂ based ceramics doped with 1.0 wt.% La^{3+} and sintered at 1300°C (d), 1400°C (e) and 1500°C (f) and of SnO₂ based ceramics doped with 1.0 wt.% V^{5+} and sintered at 1300°C (g), 1400°C (h) and 1500°C (i) / *Imagini SEM ale ceramicilor pe bază de SnO₂ sinterizate la 1300°C (a), 1400°C (b) şi 1500°C (c), ale ceramicilor pe bază de SnO₂ dopat cu 1,0 % grav. La^{3+} şi sinterizate la 1300°C (d), 1400°C (e) şi 1500°C (f) şi ale ceramicilor pe bază de SnO₂ dopat cu 1,0 % grav. V^{5+} şi sinterizate la 1300°C (g), 1400°C (h) şi 1500°C (i).*

Fig. 4 exhibits the SEM images captured on the fracture of the final ceramics. The first row is dedicated to pure SnO₂ (Figs. 4 a, b and c), the second to La^{3+} doped samples (Figs. 4 d, e and f) and the third to V^{5+} doped specimens (Figs. 4 g, h and i); the sintering temperature increases from left to right. The evolution of the nanosized powders synthesized by the precipitation method is towards densified bodies made up of polyhedral grains with rounded edges and corners and dimensions up to more than 10 μm. Generally, the increase of the processing temperature from 1300 to 1500°C favours the granular growth and porosity reduction. Moreover, the supplementary phase announced by the X-ray diffraction (Figs. 2 and 3) is also revealed by the SEM analysis in the form of round and small particles dispersed on the surface of SnO₂ bigger grains.

Concerning the influence of the dopant proportion on the microstructure of the sintered samples, Figs. 5 and 6 highlight specific features for each case. The increase of La^{3+} concentration is accompanied by the occurrence of more secondary phase, which forms a laced architecture as a result of grains connection on a large scale (Fig. 5d). Moreover, the dopant presence modifies the grains shape and size, promoting more rounded grains, compactly packed as larger aggregates. Fig. 5e presents the EDX spectra collected on the two categories of grains and demonstrate the amassment of lanthanum in the small ones.

V^{5+} mainly affects the grains dimension of SnO₂ based ceramics doped with 0.5 or 1.0 wt.%, leading even to 10 times larger grains, while in the case of 2.0 wt.% content, the shape is also changed to more elongated grains (Fig. 6d).
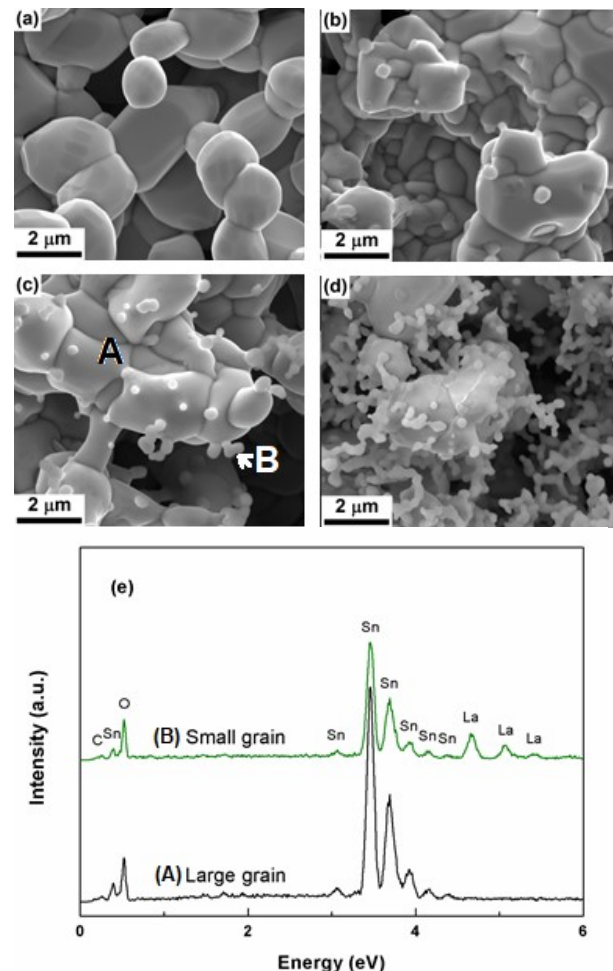

Fig. 5 - SEM images of SnO₂ based ceramics sintered at 1400°C and doped with La^{3+}: 0.0 wt.% (a), 0.5 wt.% (b), 1.0wt.% (c) and 2.0 wt.% (d), and EDX spectra obtained on the sample doped with 1.0wt.% La^{3+} / *Imagini SEM ale ceramicilor pe bază de SnO₂ sinterizate la 1400°C şi dopate cu La^{3+}: 0,0 % grav. (a), 0,5 % grav. (b), 1,0 %grav. (c) şi 2,0 % grav. (d), şi spectrele EDX realizate pe proba dopată cu 1,0 grav.% La^{3+}(e).*
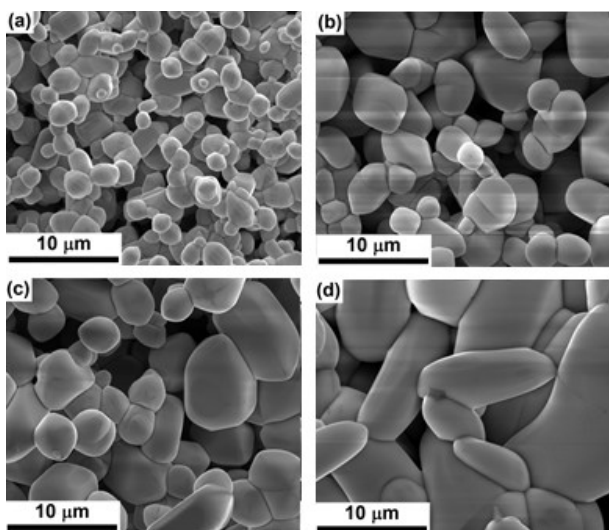
Fig. 6 - SEM images of SnO$_2$ based ceramics sintered at 1400°C and doped with V^{5+}: 0.0 wt.% (a), 0.5 wt.% (b), 1.0 wt.% (c) and 2.0 wt.% (d) / *Imagini SEM ale ceramicilor pe bază de SnO$_2$ sinterizate la 1400°C și dopate cu V^{5+}: 0,0 % grav. (a), 0,5 % grav. (b), 1,0 %grav. (c) și 2,0 % grav. (d).*

The gas sensibility of the obtained pure and doped materials was assessed for two different media: methane and isopropyl alcohol vapours. The electrical measurements were conducted after the deposition of metallic contacts on the parallel faces of the cylindrical samples by brushing a silver paste and thermally treating at 900°C. In order to eliminate the influence of bodies' size and shape, the electrical resistance was recorded both in the absence and presence of contaminants, whereupon the sensitivity was calculated, as shown in Figs. 7 and 8. La^{3+} doped ceramics do not seem to be very sensitive to methane (Fig. 7a), but in the case of isopropyl alcohol vapours, a maximum sensitivity is achieved for 1.0 wt.% concentration (Fig. 7b).

The use of V^{5+} as dopant for SnO$_2$ enhances its sensitivity to methane, the best behaviour being observed also for the proportion of 1.0 wt.% (Fig. 8a), as against the exposure to isopropyl alcohol vapours, when doping with 0.5 wt.% provides the best results (Fig. 8b).
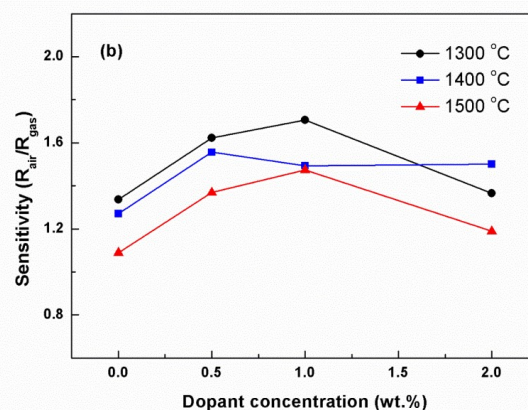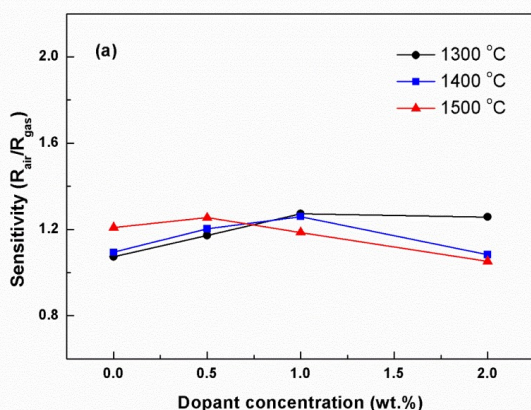

Fig. 7- Variation of sensitivity to methane (a) and isopropyl alcohol vapours (b) of SnO$_2$ based ceramics as a function of sintering temperature and La^{3+} dopant quantity / *Variația sensibilității la metan (a) și vapori de alcool izopropilic (b) a ceramicilor pe bază de SnO$_2$ în funcție de temperatura de sinterizare și cantitatea de dopant La^{3+}.*
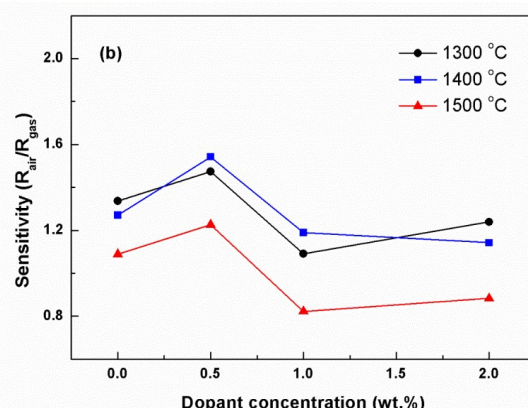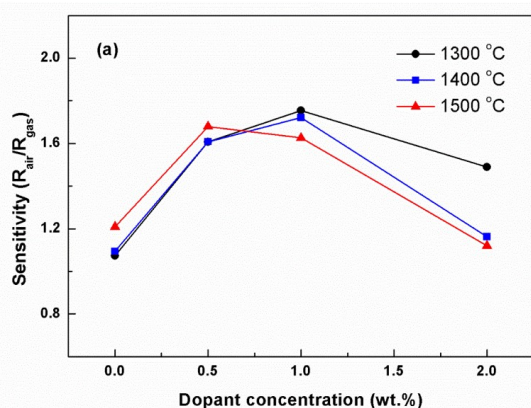

Fig. 8 - Variation of sensitivity to methane (a) and isopropyl alcohol vapours (b) of SnO$_2$ based ceramics as a function of sintering temperature and V^{5+} dopant quantity / *Variația sensibilității la metan (a) și vapori de alcool izopropilic (b) a ceramicilor pe bază de SnO$_2$ în funcție de temperatura de sinterizare și cantitatea de dopant V^{5+}.*

Analysing the implications of the sintering temperature for all discussed cases, it is obvious that a higher value for this parameter is not recommended since it naturally involves a better densification, phenomenon that has negative effects on the active surface of the sensor.

From the previous results, it is to point out the fact that by doping, not only the sensitivity, but also the selectivity of SnO_2 based sensors can be adjusted.

Conclusions

SnO_2 ceramics doped with La^{3+} or V^{5+} were obtained from precipitation derived powders through sintering at 1300, 1400 or 1500°C. The phase composition investigation revealed the appearance of a secondary phase besides the main SnO_2 tetragonal phase in the case of La^{3+} doped samples. Both the dopant concentration and sintering temperature influence the density and morphology of the resulted materials, which subsequently affect the gas sensor response. In general, a doping proportion of 0.5 - 1.0 wt% and a thermal treatment at lower temperatures are indicated so as to attain appropriate features for the field of sensors. La^{3+} improves the behaviour of SnO_2 based ceramics in the presence of isopropyl alcohol vapours, while V^{5+} has a beneficial effect in the case of methane atmosphere.

The advantages of the reported sensors, such as: simple fabrication from inexpensive precursors, high operating temperature and wear resistance, make them suitable candidates for applications in gas detection for environmental, industrial and domestic purposes.

REFERENCES

1. X. Liu, S. Cheng, H. Liu, S. Hu, D. Zhang and H. Ning, A survey on gas sensing technology, Sensors, 2012, **12**, 9635.
2. G.F. Fine, L.M. Cavanagh, A. Afonja and R. Binions, Metal oxide semi-conductor gas sensors in environmental monitoring, Sensors, 2010, **10**, 5469.
3. G. Neri, First fifty years of chemoresistive gas sensors, Chemosensors, 2015, **3**, 1.
4. A. Mirzaei, S.G. Leonardi and G. Neri, Detection of hazardous volatile organic compounds (VOCs) by metal oxide nanostructures-based gas sensors: A review, Ceramics International, 2016, **42**, 15119.
5. V.E. Bochenkov and G.B. Sergeev, Sensitivity, selectivity, and stability of gas-sensitive metal-oxide nanostructures, in Metal oxide nanostructures and their applications, Eds. A Umar and Y.B. Hahn, 2010, **3**, 31.
6. C. Wang, L. Yin, L. Zhang, D. Xiang and R. Gao, Metal oxide gas sensors: Sensitivity and influencing factors, Sensors, 2010, **10**, 2088.
7. S. Das and V. Jayarman, SnO₂: A comprehensive review on structures and gas sensors, Progress in Materials Science, 2014, **66**, 112.
8. Q.H. Wu, J. Li and S.G. Sun, Nano SnO₂ gas sensors, Current Nanoscience, 2010, **6**, 525.
9. C. Busuioc, A. Evanghelidis, C. Florica and I. Enculescu, Influence of preparation steps on the properties of electrospun ZnO fibers, Digest Journal of Nanomaterials and Biostructures, 2014, **9**, 1569.
10. W. Maziarz, A. Kusior and A. Trenczek-Zajac, Nanostructured TiO₂-based gas sensors with enhanced sensitivity to reducing gases, Beilstein Journal of Nanotechnology, 2016, **7**, 1718.
11. S. Elouali, L.G. Bloor, R. Binions, I.P. Parkin, C.J. Carmalt and J.A. Darr, Gas sensing with nano-indium oxides (In₂O₃) prepared via continuous hydrothermal flow synthesis, Langmuir, 2012, **28**, 1879.
12. N. Yamazoe, G. Sakai and K. Shimanoe, Oxide semiconductor gas sensors, Catalysis Surveys from Asia, 2003, **7**, 63.
13. O. Mounkachi, E. Salmani, M. Lakhal, H. Ez-Zahraouy, M. Hamedoun, M. Benaissa, A. Kara, A. Ennaoui and A. Benyoussef, Band-gap engineering of SnO₂, Solar Energy Materials and Solar Cells, 2016, **148**, 34.
14. P.A. Mulheran and J.H. Harding, The stability of SnO₂ surfaces, Modelling and Simulation in Materials Science and Engineering, 1992, **1**, 39.
15. Y.P. Du, J.C. Chen and J. Feng, Mechanical properties and electronic structures of various SnO₂ crystal structures, Acta Physico-Chimica Sinica, 2009, **25**, 278.
16. X. Wang, P. Ren, H. Tian, H. Fan, C. Cai and W. Liu, Enhanced gas sensing properties of SnO₂: The role of the oxygen defects induced by quenching, Journal of Alloys and Compounds, 2016, **669**, 29.
17. H.J. Snaith and C. Ducati, SnO₂-based dye-sensitized hybrid solar cells exhibiting near unity absorbed photon-to-electron conversion efficiency, Nano Letters, 2010, **10**, 1259.
18. S.Y. Lee, K.Y. Park, W.S. Kim, S. Yoon, S.H. Hong, K. Kang and M. Kim, Unveiling origin of additional capacity of SnO₂ anode in lithium-ion batteries by realistic *ex situ* TEM analysis, Nano Energy, 2016, **19**, 234.
19. H. Liu, Double-gate SnO₂ nanowire electric-double-layer transistors with tunable threshold voltage, Applied Physics Letters, 2015, **106**, 233114.
20. S.P. Kim, M.Y. Choi and H.C. Choi, Photocatalytic activity of SnO₂ nanoparticles in methylene blue degradation, Materials Research Bulletin, 2016, **74**, 85.
21. A.P.S. Isabel, C.H. Kao, R.K. Mahanty, Y.C.S. Wu, C.Y. Li, C.Y. Lin and C.F. Lin, Sensing and structural properties of Ti-doped tin oxide (SnO₂) membrane for bio-sensor applications, Ceramics International, 2017, **43**, 10386.
22. T. F. Baumann, S. O. Kucheyev, A. E. Gash and J. H. Satcher, Facile synthesis of a crystalline, high-surface-area SnO₂ aerogel, Advanced Materials, 2005, **17**, 1546.
23. W. Liu, X. Cao, Y. Zhu and L. Cao, The effect of dopants on the electronic structure of SnO₂ thin film, Sensors and Actuators B, 2000, **66**, 219.
24. H. Kose, A.O. Aydin and H. Akbulut, The effect of temperature on grain size of SnO₂ nanoparticles synthesized by sol gel method, Acta Physica Polonica A, 2014, **125**, 345.
25. T.A. Miller, S.D. Bakrania, C. Perez and M.S. Wooldridge, Nanostructured tin dioxide materials for gas sensor applications, in Functional nanomaterials, Eds. K.E. Geckeler and E. Rosenberg, American Scientific Publishers, 2006.
26. R. Vargas-Bernal and G Herrera-Perez, Importance of the nanostructured ceramic materials on gas sensing, in Nanotechnology for optics and sensors, Ed. M. Aliofkhazraei, One Central Press, 2014.
27. P. Shankar and J.B.B. Rayappan, Gas sensing mechanism of metal oxides: The role of ambient atmosphere, type of semiconductor and gases - A review, Science Letters Journal, 2015, **4**, 126.
28. G. Korotcenkov, Handbook of gas sensor materials: Properties, advantages, and shortcomings for applications, Volume 1: Conventional approaches, Springer, New York, 2013.
29. G. Korotcenkov, Handbook of gas sensor materials: Properties, advantages, and shortcomings for applications, Volume 2: New trends and technologies, Springer, New York, 2014.
30. A. Tricoli, M. Graf and S.E. Pratsinis, Optimal doping for enhanced SnO₂ sensitivity and thermal stability, Advanced Functional Materials, 2008, **18**, 1969.
31. C. Li, W. Wei, T. Xia, H. Wang, Y. Zhu and Y. Song, La-doped SnO₂: Synthesis and its electrochemical property, Journal of Rare Earths, 2010, **28**, 161.
32. C. Fu, J. Wang, M. Yang, X. Su, J. Xu and B. Jiang, Effect of La doping on microstructure of SnO₂ nanopowders prepared by co-precipitation method, Journal of Non-Crystalline Solids, 2011, **357**, 1172.
33. G.T. Ang, G.H. Toh, M.Z.A. Bakar, A.Z. Abdullah and M.R. Othman, High sensitivity and fast response SnO₂ and La-SnO₂ catalytic pellet sensors in detecting volatile organic compounds, Process Safety and Environmental Protection, 2011, **89**, 186.
34. C. Jinga, E. Andronescu, S. Jinga, A. Ioachim, L. Nedelcu and M.I. Toacsan, Synthesis and characterization of doped Ba(Mg₁/₃Ta₂/₃)O₃ ceramics, Journal of Optoelectronics and Advanced Materials, 2010, **12**, 282.
35. S.I. Jinga, S. Stoleriu and C. Busuioc, Microwave dielectric properties of Ba(Zn₁/₃Ta₂/₃)O₃ ceramics doped with Nb₂O₅, MnO₂ or V₂O₃, Materials Research Bulletin, 2012, **47**, 3713.
36. J. Sukunta, A. Wisitsoraat, A. Tuantranont, S. Phanichphant and C. Liewhiran, Highly-sensitive H₂S sensors based on flame-made V-substituted SnO₂ sensing films, Sensors and Actuators B, 2017, **242**, 1095.
37. C.T. Wang and M.T. Chen, Vanadium-promoted tin oxide semiconductor carbon monoxide gas sensors, Sensors and Actuators B, 2010, **150**, 360.
38. A.D. Busuioc, R. Enuta, S. Stoleriu, O. Oprea, T. Visan, SnO₂ powders doped with La³⁺ or V⁵⁺, Romanian Journal of Materials, 2017, **47**, xxx.
39. C. Mrabet, A. Boukhachem, M. Amlouk and T. Manoubi, Improvement of the optoelectronic properties of tin oxide transparent conductive thin films through lanthanum doping, Journal of Alloys and Compounds 2016, **666**, 392.

****